

A turbulent spot in a two-dimensional duct

By M. SOKOLOV

Department of Fluid Mechanics & Heat Transfer,
Tel Aviv University, Tel Aviv, 69978, Israel

R. A. ANTONIA AND A. J. CHAMBERS

Department of Mechanical Engineering, University of Newcastle,
NSW, 2308, Australia

(Received 31 August 1984 and in revised form 21 November 1985)

A turbulent spot is induced by a spark triggered in one of the laminar boundary layers in the entrance region of a two-dimensional duct flow. The development of the spot is studied using ensemble-averaged velocity and wall shear stress in the plane of symmetry of the spot. Following an initial growth of the spot, the potential-flow field associated with this spot triggers a second spot on the opposite wall of the duct. This new spot propagates at the same convection velocity as the original spot and grows until the turbulent regions occupied by the two spots completely fill the width of the duct. This transition mechanism differs significantly from that observed for a plane Poiseuille flow, where the spot fills the duct almost immediately after it is generated.

1. Introduction

A considerable amount of experimental work has been devoted to the study of a turbulent spot that develops in a laminar boundary layer. A recent review of the present state of knowledge of turbulent spots has been given by Riley & Gad-el-Hak (1984) and here we recall only briefly some of the salient results. One motivation for the recent attention to the spot has been the interest aroused by the study of coherent structures in a wide variety of turbulent shear flows. The original view (e.g. Coles & Barker 1975; Cantwell, Coles & Dimotakis 1978) that a spot represents an orderly structure, which may be considered as a basic building block of a turbulent boundary layer, has been altered in the light of the more recent experimental evidence which suggests that a spot consists of several coherent structures. The evidence includes flow-visualization results (Matsui 1980; Gad-el-Hak, Blackwelder & Riley 1981; Perry, Lim & Teh 1981) and observations of simultaneous temperature or velocity signals obtained with an array of cold or hot wires (Antonia *et al.* 1981*a, b*; Wygnanski, Zilberman & Haritonidis 1982).

Although definitive experiments are still required, the structures seem to bear considerable similarity to those observed (e.g. Head & Bandyopadhyay 1981) in a turbulent boundary layer. There certainly seems little doubt that, over a substantial region of the spot, quantities such as the mean velocity and turbulence-intensity profiles (e.g. Riley & Gad-el-Hak 1984) are similar to those in a turbulent boundary layer. Aspects of the spot that have been studied include the rates of spread in the spanwise and lateral (normal to the wall) directions, ensemble-averaged velocity and temperature distributions (e.g. Wygnanski, Sokolov & Friedman 1976; Antonia *et al.* 1981*a*), the influence of pressure gradient (Wygnanski, 1981; Narasimha *et al.* 1984*a*; Narasimha, Subramanian & Badri Narayanan 1984*b*), the potential field associated

with the spot (Van Atta *et al.* 1982) and the influence of Reynolds number (Sokolov, Antonia & Chambers 1980; Wagnanski *et al.* 1982).

A study (Carlson, Widnall & Peters 1982) has also been made of the evolution of a spot in plane Poiseuille flow†. Although the general geometry of the spot was similar to that observed in a boundary layer, several differences were noted. For example, Carlson *et al.* found that the spot, triggered by a pulse of fluid, expands into the flow with a half-angle of about 8° while the leading ledge of the spot travels at a convection velocity of about 0.6 times the centreline velocity. Corresponding values in a boundary layer are 10° – 11° and about 90% of the free-stream velocity (Wagnanski *et al.* 1976). Carlson *et al.* also noted that the spot split into two distinct spots near the end of their duct. Such splitting has not been observed in a boundary layer but the possibility of generating new spots at the wings of old spots has been noted by Wagnanski, Haritonidis & Kaplan (1979).

The present investigation considers the evolution of a spot introduced in the thin laminar boundary layer in the entrance region of a duct. There were two main reasons for carrying out this study. It was expected that the initial evolution of the spot should essentially reflect that observed in a boundary layer but that this evolution would eventually be affected by the bounded geometry of the flow. The documentation of the spot evolution and comparison with previous results in the boundary layer and plane Poiseuille flow seemed of interest. A second more important motivation stemmed from the observation (Antonia *et al.* 1981*a*; Van Atta *et al.* 1982) that the velocity perturbation associated with the induced flow field of the spot could be observed to a distance of about 15 spot heights from the plate. Associated with this perturbation is a pressure distribution characterized by a favourable pressure gradient followed by an adverse pressure gradient. As the disturbance or elapsed time from the perturbation increases, the magnitude of the adverse pressure gradient may be sufficient to trigger transition on the opposite wall of the duct. The present measurements corroborate the existence of a second spot there. The streamwise evolution of the two spots is documented in §3 using contours of ensemble-averaged velocity distributions and in §4 using convection velocities inferred from wall-shear-stress signals.

2. Experimental details and flow conditions

The duct used for the investigation has a working section of length 7.3 m, height 0.76 m and width $h = 66$ mm. The aspect ratio (height to width) is 11.5. Air was supplied to the working section via a centrifugal blower driven with a thyristor-controlled d.c. motor, a two-stage diffuser, a screen box, settling chamber and a 9:1 two dimensional contraction. The working-section walls were constructed with 19 mm thick Perspex panels rigidly fixed in position using aluminium channels at the top and bottom and vertical steel braces for the sides. During assembly of the Perspex panels, care was taken to ensure that all joints between adjoining Perspex panels were aerodynamically smooth. After necessary adjustments and alignments, the maximum variation in the width h was found to be $\pm 1.8\%$ over the complete length of the duct. Holes of 0.33 mm diameter were drilled at 0.3 m intervals along the working section to enable measurements of the static-pressure distribution to be made.

The spot was generated by discharging a spark, 0.49 m from the start of the

† Recently, Nishioka & Asai (1985) introduced relatively strong disturbances, using a cylinder or a periodic jet from a wall orifice, into a plane Poiseuille flow and noted the appearance of high-frequency bursts which they ascribed to turbulent spots, as visualized by Carlson *et al.* (1982).

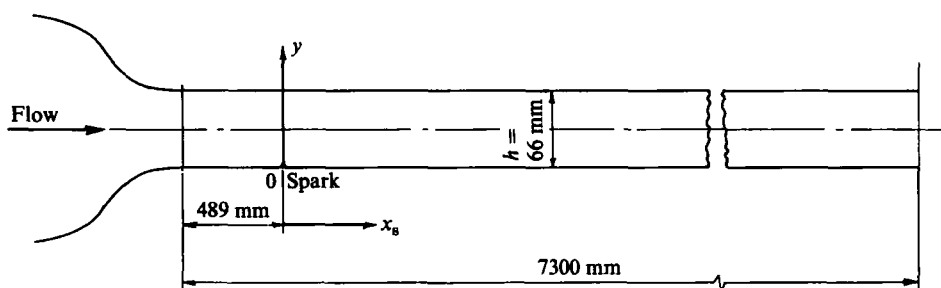


FIGURE 1. Working section of duct and coordinate axes.

working section (see figure 1), between the tips of two sewing needles which protruded about 1 mm in a direction normal to the wall and were separated in the spanwise z -direction by about 1 cm†. The centre of the gap between the needles was located on the centreline ($z = 0$) of the working section. A square-wave generator was used to trigger a capacitor-discharge (automotive) ignition system as in the experiments of Wygnanski *et al.* (1976). The frequency of the square wave used to trigger the spark-discharge unit was kept fixed for measurements at a particular value of x_s (measured from the spark); its magnitude was decreased from 2 Hz at $x_s/h = 3.6$ to 0.3 Hz at $x_s/h = 63.3$. The frequency was changed so that no more than one spot was generated between the spark and measuring location.

Simultaneous measurements were made of the wall shear stress τ with a hot film, and longitudinal velocity fluctuations U with two hot wires separated in the y -direction by about 19 mm. The hot film (DISA 55A93 miniature probe 0.75×0.15 mm) was deposited on the end of a 2.1 mm diameter cylindrical plug. This plug was mounted flush with the surface of a standard instrumentation disk, of 0.1 m diameter. A traversing mechanism, with a least count of 0.01 mm, on which the hot wires were mounted, was also attached to this disk, which could be moved to 17 different locations along the length of the duct.

Platinum-10% Rhodium hot wires (diameter = 5 μm , length ≈ 0.37 mm) were operated to an overheat ratio of 1.8 with constant-temperature anemometers (DISA 55M01). The hot film was operated with a DISA 55M01 anemometer with an overheat ratio of 1.2. Signals from the film and wires were recorded after being passed through 44D26 signal conditions (hot wires) and a buck-and-gain amplifier (hot film) on a HP3960A four-channel FM tape recorder at a speed of 95.2 mm/s. The square-wave trigger signal for the spark-discharge unit was also recorded and used to trigger and synchronize the digitizing operation. The analogue signals were played back at the recording speed and digitized using a 12-bit A-D converter at a sampling frequency ranging between 4000 and 600 Hz, depending on the value of x_s , such that each spot signature contained 1024 samples.

Calibration of the hot wires was carried out in the potential core of a plane jet over a range of velocities corresponding to those encountered in the experiments. The hot film was calibrated in the same duct but under fully developed turbulent-flow conditions. The average wall shear stress was determined from the measured constant pressure gradient and also from a Preston tube located at the same streamwise location as the hot film.

† Although this distance is larger than in the experiments of Antonia *et al.* (1981), Wygnanski *et al.* (1976) tried several spark geometries and found that the spot was independent of the disturbances that generated it.

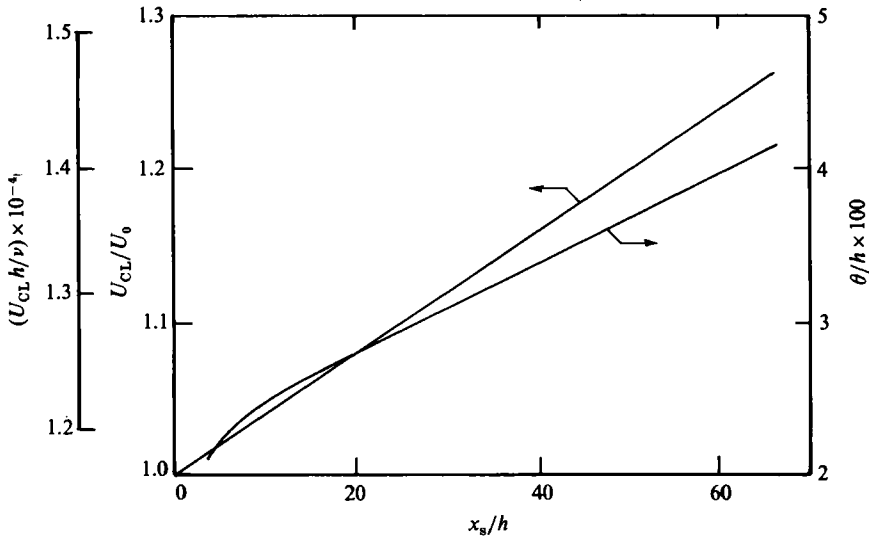


FIGURE 2. Variation of centreline velocity, Reynolds number and momentum thickness of laminar boundary layer.

Experiments were conducted only when other apparatus in the laboratory was not in use to minimize the effect of background vibration and therefore reduce the possibility of natural transition. All measurements were made at $z = 0$ only for a nominal velocity at the entrance to the working section of 2.6 m/s. This velocity was monitored throughout the experiments by monitoring the pressure difference across the two-dimensional contraction.

At the location of the spark the centreline velocity U_0 is approximately 2.65 m/s and the Reynolds number $Re \equiv U h / \nu$ is about 11600. The Reynolds-number variation along the duct is shown in figure 2. The entry length required (see Schlichting 1979, p. 185) for the laminar velocity profile to become fully developed is approximately $0.04h Re$ or $466h$, which is significantly greater than the length of the duct ($\approx 111h$). The streamwise variations (figure 2) of the centreline velocity U_{CL} and the momentum thickness θ of the boundary layer are, within the experimental uncertainty, approximately linear over a significant range of x_s ; θ/h appears to increase parabolically for $x_s/h \lesssim 20$. The favourable pressure gradient associated with the distribution of U_{CL}/U_0 in figure 2 is small. At $x_s/h = 63.3$, the static pressure relative to that at the spark location is $-0.13 \rho U_0^2$.

Howarth (see Schlichting 1979, p. 173) obtained a family of solutions to the boundary-layer equations for laminar flow which related to a potential flow given by $U_{CL} = U_0 - ax$. This streamwise variation of U_{CL} is consistent with the measurements in figure 2. The measured static pressure gives $a/U_0 \approx 0.031 \text{ m}^{-1}$ (or $ax/U_0 = -0.1$ for $x/h = 49$). The Howarth solution is compared with measured distributions of U/U_{CL} , plotted in terms of y/θ , in figure 3. For $x_s/h < 10$, the Blasius solution, also shown in figure 3, should more correctly predict the form of the velocity distribution, while for $30 < x_s/h < 60$, the flow on this solution with $ax/U_0 = -1$ should be more relevant than that of Blasius. The data in figure 3 are consistent with these expectations.

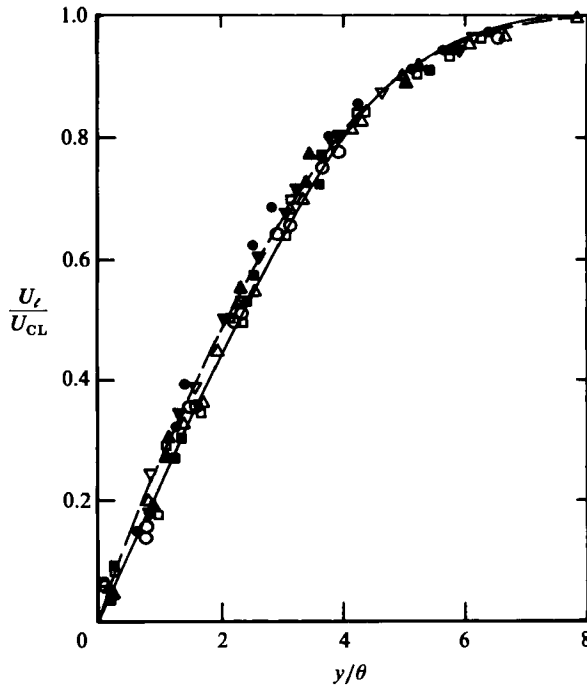


FIGURE 3. Measured laminar velocity profiles along the duct and comparison with calculation. —, Blasius; ---, Howarth; ○, $x_s/h = 3.6$; □, 7.8; △, 17.1; ▽, 26.3; ●, 35.5; ▼, 44.8; ■, 54.0; ▲, 63.3. $\alpha x/U_0 = -0.1$.

3. Evolution of spot and interaction with opposite wall

Ensemble averages of the instantaneous U and τ signals were obtained with reference to the firing of the spark. For practical reasons, the averaging was started on the computer after a certain time had elapsed following the spark (this time was estimated by first observing time traces of U and τ). Ensemble averages were formed using 200 realizations†. As x_s increased, the firing frequency of the spark generator was decreased to allow sufficient time for relaxation to laminar conditions between successive firings. The record duration was increased accordingly to permit computations to be made on the same number of realizations.

Instantaneous velocity and shear-stress fluctuations were decomposed as follows

$$U = U_\ell + \tilde{U} + u,$$

$$\tau = \tau_\ell + \tilde{\tau} + \tau',$$

where the subscript ℓ refers to the value in the laminar flow and \tilde{U} and $\tilde{\tau}$ are the ensemble-averaged values of $U - U_\ell$ and $\tau - \tau_\ell$ respectively. With angular brackets denoting ensemble averages, \tilde{U} and $\tilde{\tau}$ represent ensemble-averaged disturbances relative to undisturbed laminar conditions:

$$\tilde{U} = \langle U \rangle - U_\ell,$$

$$\tilde{\tau} = \langle \tau \rangle - \tau_\ell.$$

By definition, $\langle u \rangle$ and $\langle \tau' \rangle$ are equal to zero.

† The same number was used by Antonia *et al.* (1981*a*) and Wynanski *et al.* (1982).

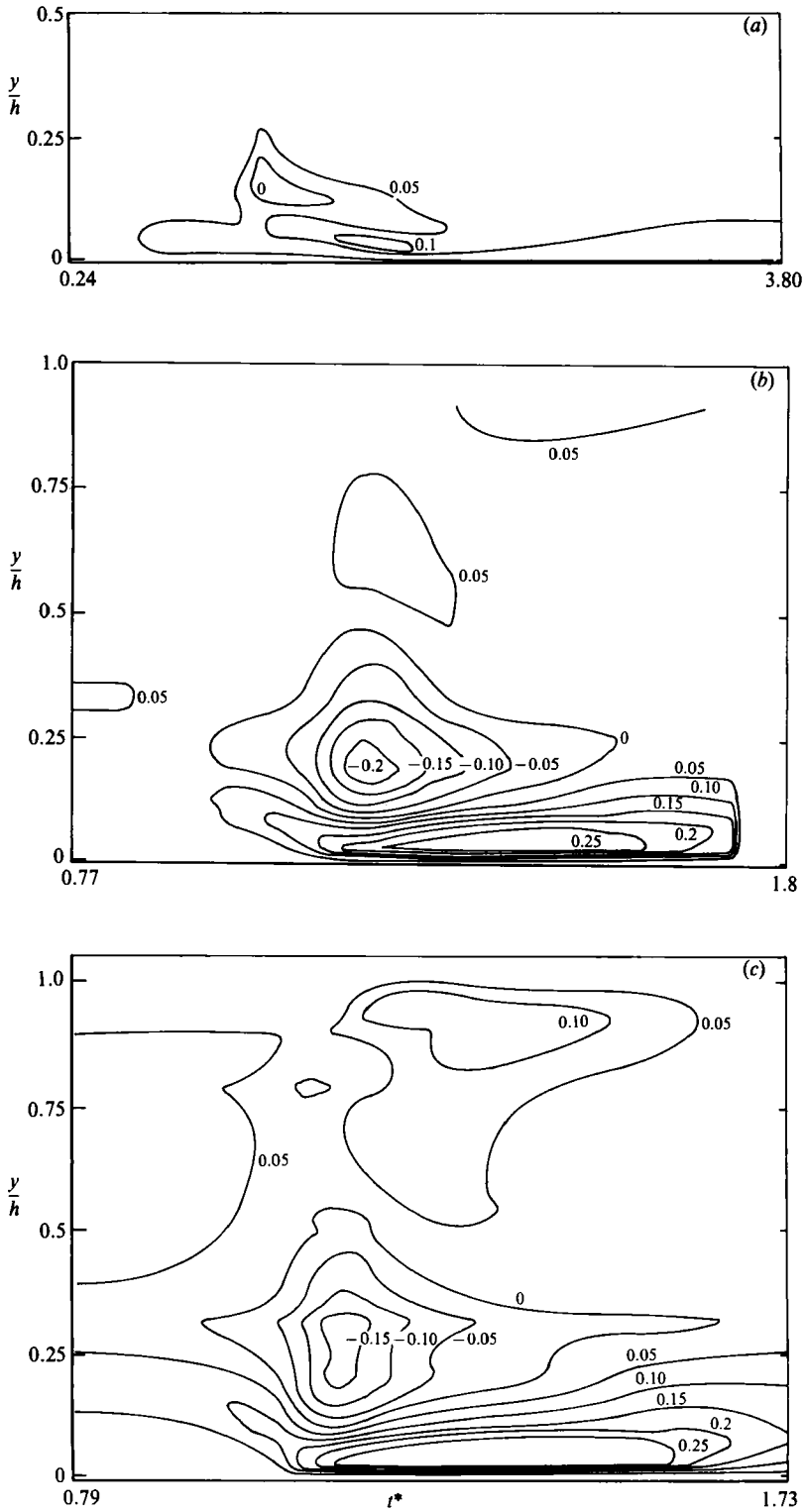


FIGURE 4(a, b, c). For caption see facing page.

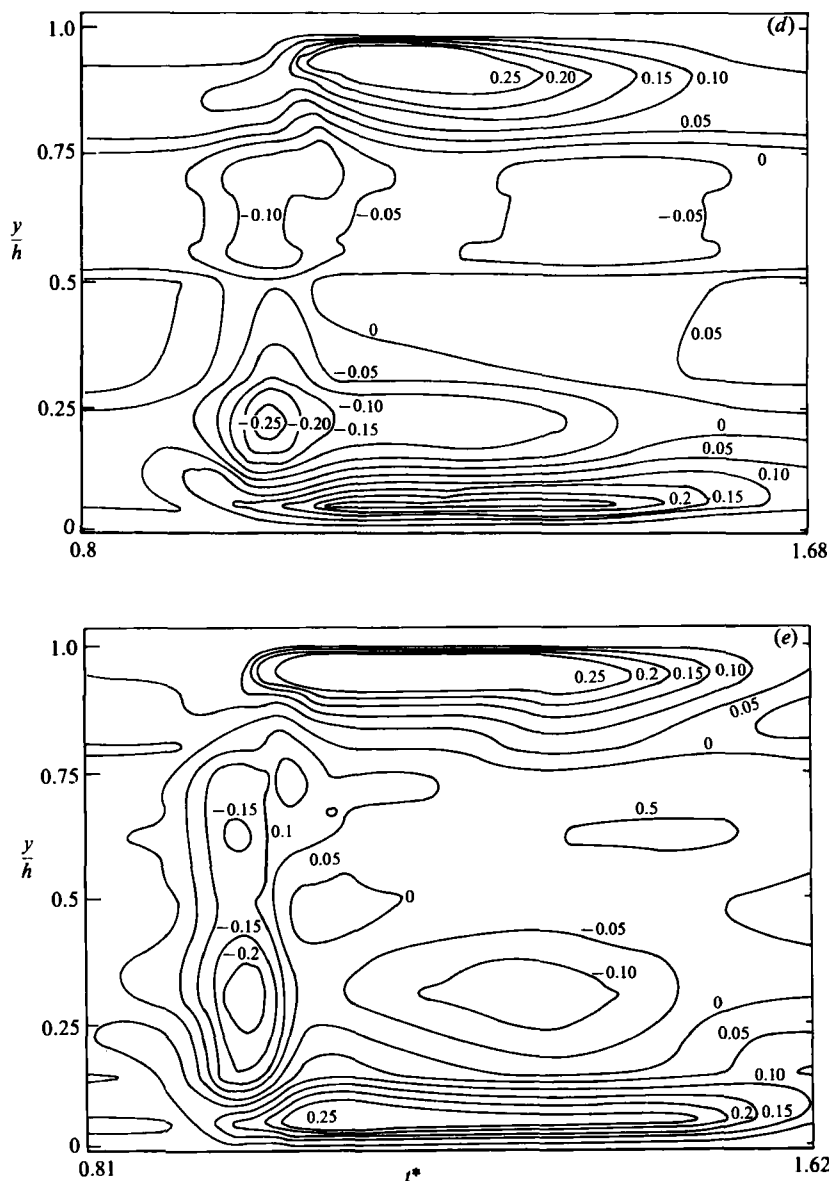


FIGURE 4. Contours of constant velocity disturbance \tilde{U}/U_{CL} at five streamwise stations. (a) $x_s/h = 3.6$; (b) 26.3; (c) 35.5; (d) 44.8; (e) 63.3.

Contours of constant \tilde{U}/U_{CL} , in the (y, t) -plane, were computed at eight values of x_s . Results at only five of these are shown in figure 4 as they convey a sufficiently representative picture for the streamwise evolution of the disturbance caused by the spot. For the purpose of presentation, the time t from the spark has been normalized by the reference velocity U_0 and x_s such that $t^* = tU_0/x_s^\dagger$. This normalization is similar to that used in previous investigations in the boundary layer (e.g. Cantwell *et al.* 1978). The value of y has been normalized by the duct width h . For the

† It should be recalled that the contours in figure 4 do not represent instantaneous cuts in the (y, t) -plane. They are strictly ensemble averages relative to the spark.

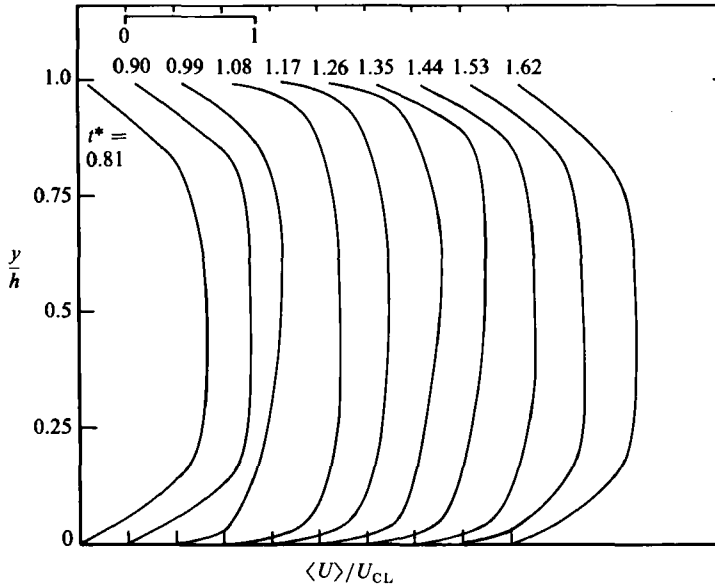


FIGURE 5. Profiles of $\langle U \rangle / U_{CL}$ for different values of t^* at $x_s/h = 63.3$.

boundary-layer spot, the relevant non-dimensional ordinate is y/δ (see Sokolov *et al.* 1980; Wygnanski *et al.* 1982) where $\delta(x_s)$ is the thickness of a turbulent boundary layer with effectively the same origin as the spot. In the present flow, the spot development is eventually affected by the presence of both walls and y has therefore been normalized by the duct width h .

The behaviour of the contours in figure 4 exhibits all the characteristics already reported in the literature (e.g. Wygnanski *et al.* 1976; Antonia *et al.* 1981*a*) for a spot in a laminar boundary layer with zero pressure gradient. If attention is first focused on the lower half of the duct ($y/h < 0.5$), a positive value of \tilde{U}/U_{CL} close to $y = 0$ is quickly replaced by negative values of larger y . At $x_s/h = 3.6$ few measurements were made in the upper half of the duct ($y/h > 0.5$) as the potential-flow disturbance associated with the spot could not be observed in this region of the duct. As x_s/h increases, the potential disturbance due to the spot penetrates the upper half of the duct. At $x_s/h = 35.5$, the positive $-\tilde{U}/U_{CL}$ contours near $y = h$ reveal a second spot on the opposite wall of the duct. Contours of \tilde{U}/U_{CL} (figure 4) at $x_s/h = 44.8$ indicate all the characteristic features of a developing spot. At this station, the contour $\tilde{U}/U_{CL} = -0.05$ associated with the second spot has reached the duct centreline. Negative $-\tilde{U}/U_{CL}$ contours on the opposite sides of the centreline are not symmetric. The magnitude of the maximum velocity defect associated with the second spot is smaller than that obtained for the first spot, implying that the second spot is not as strong as the first. Closer symmetry with respect to the centreline is displayed at $x_s/h = 63.3$. Distributions of $\langle U \rangle / U_{CL}$ for several specific values of t^* at this station (figure 5) also display this symmetry. They further indicate an increase in the velocity gradient at both walls as the spots arrive at this station. Distributions at small ($t^* \lesssim 0.9$) and large ($t^* \gtrsim 1.53$) times correspond to laminar conditions in the duct and the velocity gradients are accordingly smaller than during the passage of the spot.

It is of interest to follow the streamwise evolution of the disturbance \tilde{U} along the

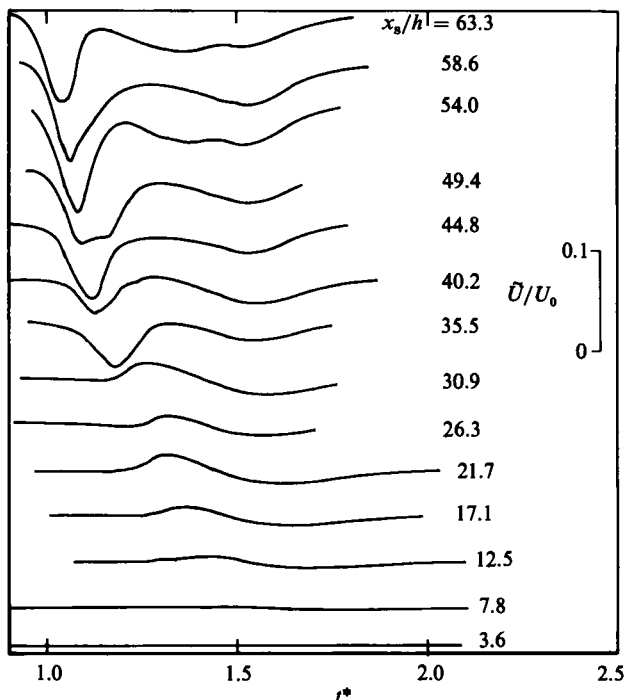


FIGURE 6. Variation with x_s of velocity disturbance \bar{U}/U_{CL} at $y \approx \frac{1}{2}h$.

duct. Figure 6 represents distributions of \bar{U}/U_0 on the centreline of the duct. The potential disturbance of the first spot can initially be seen at $x_s/h = 7.8$. It subsequently increases in amplitude reflecting the growth of this spot. The potential signature at $x_s/h = 21.7$ consists of a positive perturbation followed by a negative one, as previously observed (Van Atta *et al.* 1982) for sufficiently large heights above a boundary-layer spot. The increase in amplitude suggests an increase in the magnitudes of the favourable and adverse pressure gradients associated with the potential disturbance. At $x_s/h = 35.5$, the signature observed at smaller values of x_s/h is now preceded by a negative perturbation, which increases in magnitude with a further increase in x_s/h .

The possibility that the acoustic disturbance introduced by the spark may be responsible for the second spot seemed unlikely in view of the relatively large streamwise distance ($\approx 35h$) from the spark at which this spot is first observed. This assertion was confirmed by replacing the spark with a small (diameter = 1 mm, height ≈ 5 mm) cylindrical pin. Although the pressure disturbance due to the pin may not be negligible, it should be less significant than that caused by the spark. The pin introduced a train of spots into the laminar boundary layer. Transition occurred at the opposite wall at about the same distance as with the spark. This observation rules out the possibility of an acoustically induced second spot but also reinforces the speculation that the second spot is triggered by the unsteady pressure field associated with the first spot. The magnitude of $\partial\bar{p}/\partial x$, where \bar{p} is the ensemble-averaged pressure disturbance due to the first spot, at $x_s \approx 35h$ could, in principle, be estimated via the linearized unsteady Bernoulli equation, a procedure followed by Cantwell *et al.* (1978). Using a conical similarity transformation, these authors obtained a universal pressure coefficient associated with the spot. However,

Antonia *et al.* (1981 *b*) pointed out that their measurements in the potential flow above the spot indicated an important variation with y of the potential-velocity field, thus ruling out a universal pressure distribution. Because of this ambiguity, we have not attempted to calculate the pressure field associated with the main spot. Also, before a quantitative criterion for the onset of the second spot can be developed, more information is needed about the influence of pressure gradients, both favourable and adverse, on transition.

4. Wall-shear-stress distributions and convection velocities

The shear-stress signal obtained with the hot film was ensemble averaged using the same procedure that was applied to the hot-wire signals. Distributions of $\bar{\tau}$ are shown in figure 7(*a*) for different values of x_s/h . To identify the origin of the second spot more precisely than was possible with the information discussed in the previous section, it seemed desirable to consider the shear-stress signals on the other wall of the duct. This would also enable the convection velocity of the spot to be estimated. It was experimentally more convenient to shift the spark to the surface $y = h$ rather than install the film there. For the ensemble-averaged shear-stress distributions in figure 7(*b*), the spark was located at $y = h$ and a distance of 508.8 mm from the duct entrance.

At sufficiently large x_s , the ensemble-averaged distributions in figures 7(*a*) and *b*) exhibit a characteristic signature: the shear stress increases relatively sharply at the leading edge of the spot and then more gradually until it reaches a maximum value near the trailing edge of the spot. This is followed by an almost exponential relaxation towards the laminar state. The characteristic shear-stress signature is similar to that which can be inferred from the behaviour of ensemble-averaged velocity distributions obtained from a hot wire located close to the wall (e.g. see Wygnanski *et al.* 1976 for a fully developed spot and Amini & Lespinard 1982 for the later stages of an incipient spot in a laminar boundary layer). A similar signature was obtained with a wall hot film by Rajagopalan & Antonia (1980) during natural transition in the entrance region of a duct. Tani (1982) refers to Handa's measurements of a spot in a laminar boundary layer over a flat plate for which the wall shear stress attains a maximum at $x_s/U_\infty t = 0.52$ or $U_\infty t/x_s = 1.92$. The present measurements indicate that a maximum value of wall shear stress is attained with $1.7 < t^* < 2.0$, in reasonable agreement with Handa's measurements.

The relatively sharp rise† in $\bar{\tau}$ near the leading edge of the spot suggests a quite accurate means of determining the convection velocity of the leading edge of the spot. The leading-edge arrival time was identified here with the time at which $\bar{\tau}$ first reaches 5% of its maximum value. The trailing-edge arrival time was defined as the time when $\bar{\tau}$ first decreases to below 50% of its maximum value. Arrival times, as a function of x_s , of leading and trailing edges are shown in figures 8(*a*, *b*). For $x_s \gtrsim 1.65$ m ($x_s/h \gtrsim 25$), the data for leading- and trailing-edge arrival times for the first spot (figure 8*a*) vary linearly with x_s , indicating constant convection velocities of the leading and trailing edges. Although the definitions of leading- and trailing-edge arrival times are arbitrary, the resulting convection velocities were insensitive to the precise definitions. The intersection of the straight lines in figure 8(*a*) defines a virtual

† Note that this rise is degraded by the ensemble averaging. Much sharper rise times are observed on individual realizations (this was also evident in oscillograms of U obtained close to the surface by Schubauer & Klebanoff 1956); arrival times estimated from a number of individual realizations were, however, in good agreement with those estimated from ensemble averages.

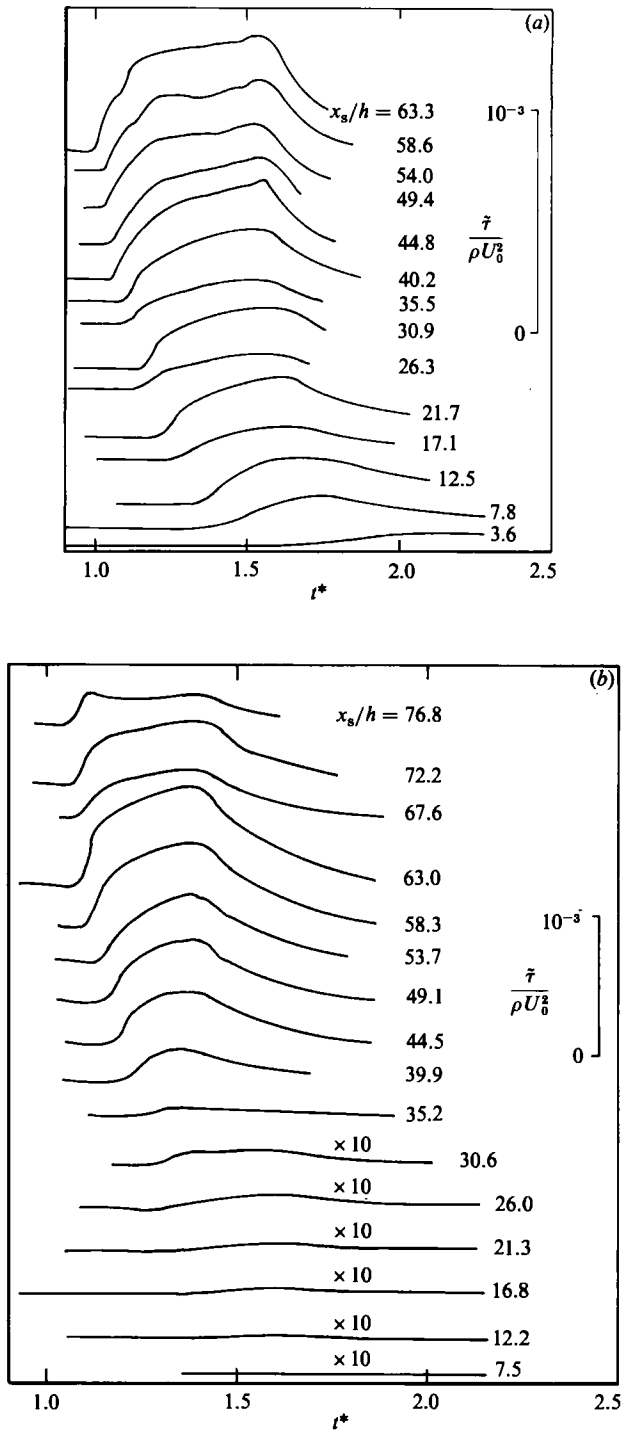


FIGURE 7. Ensemble-averaged wall-shear-stress disturbances at $y = 0$ and different values of x_s .
 (a) spark at $y = 0$; (b) spark at $y = h$.

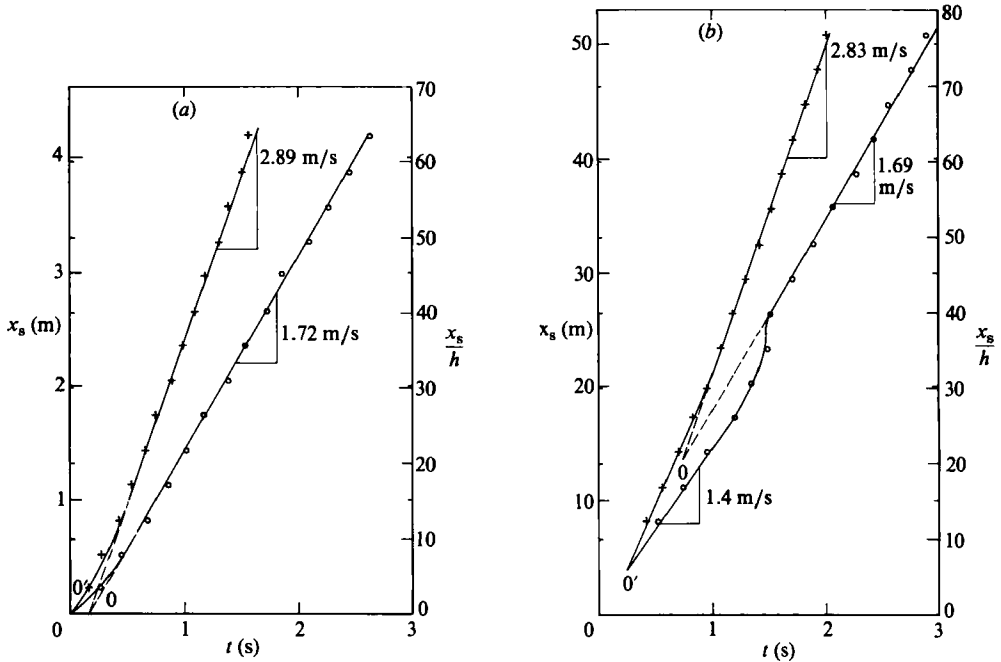


FIGURE 8. Arrival times of leading and trailing edges, based on distributions of $\langle \tau \rangle$ at $y = 0$ and different values of x_s . (a) spark at $y = 0$; (b) spark at $y = h$.

origin at $x_s = 0$ and $t = 0.16$ s. Figure 8(b) indicates that the convection velocity of the second spot is approximately constant for $x_s \gtrsim 2.3$ m ($x_s/h \gtrsim 35.5$). The leading and trailing edges of this second spot travel with the same velocities as the leading and trailing edges of the first spot, at least to within the experimental uncertainty, estimated to be about $\pm 1\%$. A comparison of figures 8(a) and (b) indicates that the leading edge of the first spot lies downstream of the leading edge of the second spot by a distance of $5h$ (the angle that the line joining leading edges extends to the wall is 11.3°). On the other hand, since the second spot is only at an early stage of development, its trailing edge is detected, at any given time, before the trailing edge of the first spot. The intersection of the lines in figure 8(b) locates the virtual origin at $x_s = 20.6h$ (with $t^* = 1.46$). It is of interest to consider the data for $x_s \lesssim 2.3$ m, which are associated with the incipient second spot or, at the smallest values of x_s , with the potential disturbance due to the first spot. The data suggest that this disturbance is first detected at $x_s = 0.8$ m ($x_s/h \approx 12.2$). This small value of x_s is consistent with the rapidity with which the potential disturbance of the first spot propagates to the other wall. Figure 8(b) indicates that a relatively sudden acceleration occurs, especially at the trailing edge, near $x_s/h = 35.5$. This acceleration is necessary since the convection velocity of the potential disturbance at $y = h$ or of the 'incipient second spot' should reflect primarily the convection velocity of the 'incipient first spot' and the latter convection velocity is significantly smaller than the convection velocity of the fully developed first spot.

The constancy of the convection velocity in figures 8(a, b) implies an interesting relationship between the present spot or spots and the spot in a laminar boundary layer or in plane Poiseuille flow. In a laminar boundary layer, the convection velocity of the leading edge, in the plane of symmetry of the spot, is $0.89U_\infty$ (Wyganski *et al.* 1976, 1982). Wyganski *et al.* (1976) reported a value of $0.5U_\infty$ for the trailing

edge of the spot; more recently Wygnanski *et al.* (1982) obtained a value of $0.57U_\infty$ †. In plane Poiseuille flow, Carlson *et al.* (1982) found that the front of the spot propagates at a velocity of $0.6U_{CL}$ ‡ while the rear travels at $0.34U_{CL}$. In the present experiment, the ratio of the convection velocity of the leading edge to the centreline velocity is approximately constant and equal to 0.87 for x_s/h greater than 12. The ratio of leading-edge to trailing-edge convection velocities is 1.56 for the boundary layer, using Wygnanski *et al.*'s (1982) data, and 1.76 for plane Poiseuille flow. The present ratio of 1.68 falls between these two values. This trend suggests that the present spot behaves initially like that in a boundary-layer but, as x_s increases, its behaviour approaches that of a spot in plane Poiseuille flow. It should be noted that the Reynolds number of the boundary-layer spot increases with x_s whereas for plane Poiseuille flow the spot Reynolds number is constant. For the present spot, the Reynolds number initially increases as for that in a boundary-layer but its rate of growth must eventually decrease as the two spots share the space between the duct walls.

Since measurements were not made in the spanwise direction, we cannot comment with authority on the similarity between the development of the present spot and that in a boundary layer with zero pressure gradient. Previous work (Wygnanski 1981; Narasimha *et al.* 1985 *a*) has shown the significant effect of a favourable pressure gradient can have, through its stabilizing influence, on the spanwise growth of the spot.

The mechanism by which a turbulent spot spreads in the spanwise direction is probably the same for the boundary layer as for plane Poiseuille or the present flows. Corrsin & Kistler's (1955) suggestion that the mechanism may consist of a destabilization of the rotational flow adjacent to the spot 'in addition to a transmission of random vorticity by direct viscous action at the turbulent-laminar interface' has been elaborated further by Riley & Gad-el-Hak (1984). The observed differences in the spanwise growth between boundary-layer and plane Poiseuille flows may reflect genuine differences in the dynamics of the spots in these flows. An investigation of the spanwise growth of the spots in the present flow would be a useful extension of the present work.

5. Concluding remarks

The initial development of a turbulent spot in the laminar entrance region of a finite-aspect-ratio duct is similar to that documented for the boundary layer with zero pressure gradient. This result is based on ensemble-averaged distributions of velocity and wall shear stress. The wall shear stress increases almost continuously between the leading and trailing edges of the spot. This trend is identical to that inferred from either near-wall velocity traces measured in a spot within a laminar boundary layer or from wall-shear-stress traces measured during natural transition in the entrance region of a duct. At a distance of about 35 duct widths from the spark location, the boundary layer on the opposite duct wall undergoes transition and a second spot is formed. This new spot is not caused by the acoustic disturbance of the spark; it is speculated, however, that the adverse pressure gradient associated with the potential-flow disturbance of the first spot is sufficiently strong to induce transition on the opposite duct wall. More work on the influence of pressure gradients

† Strictly, these authors suggested this convection velocity decreases with increasing Reynolds number.

‡ Note that U_{CL} does not vary with x_s in this flow.

on transition would be required to enable a quantitative criterion for transition to be established.

The second spot propagates at the same convection velocity as the first one and grows until the turbulent regions occupied by other spots fill the cross-section of the duct. At the last measurement station, isocontours of the velocity disturbance relative to laminar conditions are nearly symmetrical with respect to the centreline of the duct. The previous scenario for the development of the first spot and its generation of and subsequent interaction with the second will also apply in the case of natural transition. However, the latter situation is not as amenable for study since many spots at different stages of development are captured at a fixed measurement station.

The results presented in this paper suggest a mechanism of transition for the entrance region of a duct which differs, at least in one important way, from that in a plane Poiseuille flow. The initiation of a turbulent spot in the entrance region of a duct eventually leads to the initiation of a second spot which grows until the turbulent regions associated with the two back-to-back spots completely fill the duct width. There is no reason to expect the turbulent spots to lose their identity after they meet. Dean & Bradshaw (1976) postulated that downstream of the merging of the opposite shear layers in a turbulent duct flow, large-eddy eruptions from one side of the centreline time-share with those from the opposite side. This postulate seems, perhaps *a fortiori*, relevant to the interaction between opposite spots near the centreline. For a plane Poiseuille flow, Carlson *et al.* (1982) found that although the spot was produced, as in the present case, by an asymmetric disturbance at one wall, the spot filled the width of the duct to within a few duct widths of the location of the disturbance. This almost-instantaneous propagation of the spot across the duct cross-section is in marked contrast to the present observations.

The authors are grateful to Dr S. Rajagopalan, Messrs D. A. Shah and R. Sankaran for their contributions to the experiments and to Dr D. Britz for his assistance with computations. A grant from the Senate Research Committee of the University of Newcastle and the support of the Australian Research Grants Scheme are acknowledged.

REFERENCES

- AMINI, J. & LESPINARD, G. 1982 Experimental study of an "incipient spot" in a transitional boundary layer. *Phys. Fluids* **25**, 1743-1750.
- ANTONIA, R. A., CHAMBERS, A. J., SOKOLOV, M. & VAN ATTA, C. W. 1981*a* Simultaneous temperature and velocity measurements in the plane of symmetry of a transitional turbulent spot. *J. Fluid Mech.* **108**, 317-343.
- ANTONIA, R. A., CHAMBERS, A. J., SOKOLOV, M. & VAN ATTA, C. W. 1981*b* On the similarity between velocity and temperature fields within a turbulent spot. In *Proc. 3rd Symp. on Turbulent Shear Flows*, Davis, pp. 10.1-10.6.
- CANTWELL, B., COLES, D. & DIMOTAKIS, P. 1978 Structure and entrainment in the plane of symmetry of a turbulent spot. *J. Fluid Mech.* **87**, 641-672.
- CARLSON, D. R., WIDNALL, S. E. & PETERS, M. F. 1982 A flow-visualization study of transition in plane Poiseuille flow. *J. Fluid Mech.* **121**, 487-505.
- COLES, D. & BARKER, S. J. 1975 Some remarks on a synthetic turbulent boundary layer. In *Turbulent Mixing in Non-reactive and Reactive Flows* (ed. S. N. B. Murthy), pp. 285-292. Plenum.
- CORRSIN, S. & KISTLER, A. L. 1955 Free-stream boundaries of turbulent flows. *NACA Rep.* 1244.
- DEAN, R. B. & BRADSHAW, P. 1976 Measurements of interacting turbulent shear layers in a duct. *J. Fluid Mech.* **78**, 641-676.

- GAD-EL-HAK, M., BLACKWELDER, R. F. & RILEY, J. J. 1981 On the growth of turbulent regions in laminar boundary layers. *J. Fluid Mech.* **110**, 73–96.
- HEAD, M. R. & BANDYOPADHYAY, P. 1981 New aspects of turbulent boundary-layer structure. *J. Fluid Mech.* **107**, 297–338.
- MATSUI, T. 1980 Visualization of turbulent spots in the boundary layer along a flat plate in a wall flow. In *Laminar–Turbulent Transition* (ed. R. Eppler & H. Fasel), pp. 288–296. Springer.
- NARASIMHA, R., DEVASIA, K. J., GURURANI, G. & BADRI NARAYANAN, M. A. 1984*a* Transitional intermittency in boundary layers subjected to pressure gradient. *Expts in Fluids* **2**, 1–6.
- NARASIMHA, R., SUBRAMANIAN, C. S. & BADRI NARAYANAN, M. A. 1984*b* Turbulent spot growth in favorable pressure gradients. *AIAA J.* **22**, 837–839.
- NISHIOKA, M. & ASAI, M. 1985 Some observations of the subcritical transition in plane Poiseuille flow. *J. Fluid Mech.* **150**, 441–450.
- PERRY, A. E., LIM, T. T. & TEH, E. W. 1981 A visual study of turbulent spots. *J. Fluid Mech.* **104**, 387–405.
- RAJAGOPALAN, S. & ANTONIA, R. A. 1980 Investigation of natural transition in the inlet region of a two dimensional duct flow. *Phys. Fluids* **23**, 1938–1948.
- RILEY, J. J. & GAD-EL-HAK, M. 1984 The Dynamics of turbulent spots. In *Fundamentals of Fluid Mechanics* (ed. S. H. Davis & J. L. Lumley). Springer.
- SCHLICHTING, H. 1979 *Boundary Layer Theory*, 7th edn. McGraw-Hill.
- SCHUBAUER, G. B. & KLEBANOFF, P. S. 1956 Contributions on the mechanics of boundary-layer transition. *NACA Rep.* 1289.
- SOKOLOV, M., ANTONIA, R. A. & CHAMBERS, A. J. 1980 A similarity transformation for a turbulent spot in a laminar boundary layer. *Phys. Fluids* **23**, 2561–2563.
- TANI, I. 1982 Three-dimensional aspects of boundary-layer transition. In *Surveys in Fluid Mechanics* (ed. R. Narasimha & S. M. Deshpande) pp. 125–144. Indian Academy of Sciences.
- VAN ATTA, C. W., SOKOLOV, M., ANTONIA, R. E. & CHAMBERS, A. J. 1982 Potential flow signature of a turbulent spot. *Phys. Fluids* **25**, 424–428.
- WYGNANSKI, I. 1981 The effect of reynolds number and pressure gradient on the transitional spot in a laminar boundary layer (ed. J. Jimenez). *Lecture Notes in Physics*, Vol. 136, pp. 304–332. Springer.
- WYGNANSKI, I., HARITONIDIS, J. H. & KAPLAN, R. E. 1979 On a Tollmien–Schlichting wave packet produced by a turbulent spot. *J. Fluid Mech.* **92**, 505–528.
- WYGNANSKI, I., SOKOLOV, M. & FRIEDMAN, D. 1976 On a turbulent “spot” in a laminar boundary layer. *J. Fluid Mech.* **78**, 785–819.
- WYGNANSKI, I., ZILBERMAN, M. & HARITONIDIS, J. H. 1982 On the spreading of a turbulent spot in the absence of a pressure gradient. *J. Fluid Mech.* **123**, 69–90.